



Numerical Experiments on Flow and Transport of Various Surfactant Solutions in the Vadose Zone

Sebnem Boduroglu, Rashid Bashir

Department of Civil Engineering – York University, Toronto, Ontario, Canada

ABSTRACT

Surfactants exist in the subsurface either naturally or as a result of anthropogenic activities related to agriculture or soil/groundwater remediation. With climate change, greywater containing large amounts of surfactants is increasingly being used in the semi-arid and arid regions. Surfactants affect soil capillarity through surface tension and contact angle changes and thus alter flow and transport characteristics of the vadose zone. The research on how flow is affected by the surfactants is very limited. Most of the conceptual and numerical models assume that flow is independent of the solute concentration, which does not provide accurate representation of the flow and transport of surfactant solutions in the unsaturated zone. This research uses a modified version of unsaturated flow and transport code Hydrus 2D, which couples flow and transport by implementing concentration dependent capillarity effects. Infiltration characteristics and flow and transport of two different surfactant solutions in the vadose zone is simulated in this research. The flow and transport of surfactants is compared with flow of water and associated transport of a conservative solute. In both cases, surfactant solutions led to notable differences in comparison to pure water and conservative solute. The differences were result of surfactant induced pressure gradients and hysteretic behavior under monotonic flow conditions. Additionally, the results also indicate that the flow and transport of surfactants is not only dependent on concentration dependent capillarity effects but also on different sorption characteristics of the surfactants. The current research will help in enhancing our understanding of the flow, transport and fate of the surfactants in the vadose zone and their possible link to future environmental problems.

RÉSUMÉ

Les agents tensioactifs existent à la surface naturellement, ou à la suite d'activations anthropiques liées à l'agriculture ou à l'assainissement des sols et des eaux souterraines. Avec le changement climatique, les eaux grises contenant de grandes quantités de tensioactifs sont de plus en plus utilisées dans les régions semi-arides et arides. Les agents tensioactifs affectent la capillarité du sol par la tension de surface et les changements d'angle de contact et modifient ainsi les caractéristiques d'écoulement et de transport de la zone Vadose. La recherche sur la façon dont le flux est affecté par les tensioactifs est très limitée. La plupart des modèles conceptuels et numériques supposent que l'écoulement est indépendant de la concentration du soluté, ce qui ne fournit pas une représentation précise de l'écoulement et du transport des solutions tensioactives dans la zone non saturée. Cette recherche utilise une version modifiée du code d'écoulement et de transport Hydrus 2D, qui accompagne l'écoulement et le transport en mettant en œuvre des effets de capillarité dépendant de la concentration. Les caractéristiques d'infiltration et le débit et le transport de deux solutions différentes tensioactives dans la zone Vadose sont simulés dans cette recherche. L'écoulement et le transport des tensioactifs sont comparés avec le flux d'eau et le transport associé d'un soluté conservateur. Dans les deux cas, les solutions tensioactives ont conduit à des différences notables par rapport à l'eau pure et au soluté conservateur. Les différences résultent des gradients de pression induits par le tensioactif et le comportement hystérétique dans des conditions d'écoulement monotones. De plus, les résultats indiquent que l'écoulement et le transport des agents tensioactifs ne dépendent pas seulement des effets de capillarité dépendant de la concentration, mais également des différentes caractéristiques de sorption des agents tensioactifs. La recherche actuelle nous aidera à mieux comprendre l'écoulement, le transport et le devenir des tensioactifs dans la zone Vadose et leur lien possible avec les problèmes environnementaux futurs.

1 INTRODUCTION

Freshwater scarcity is one of the biggest concerns for our time. As increasing population and climate change puts more pressure on existing water resources, use of grey water is becoming increasingly common in many arid and semi-arid regions of the world. Greywater refers to waste water from baths, sinks, washing machines and other kitchen appliances. In spite of the fact that greywater contains contaminants with potential environmental risks such as household chemicals, salts, oils and pathogens; it is generally assumed as 'relatively clean'. According to Eriksson et al (2003), surfactants are one of the major groups of compounds found present in greywater. In this study, the term 'surfactant' is used to specify all organic compounds that reduce the surface tension of water. Surfactants can be found in the subsurface either naturally or due to anthropogenic activities. A natural source of

surfactants in the subsurface is humic acid. Anthropogenic activities contributing to presence of surfactants in the subsurface can be agricultural or remediation related. Surfactant solutions are used for improvements to soil structure, soil erosion and infiltration (Abu-Zreig et al, 2003). Use of grey water for irrigation purposes can also contribute to the addition of surfactants to subsurface as surfactant concentrations in domestic grey water can range from 0.7 to 70 mg/L (Wiel-Shafran et al, 2006). Although there is a growing tendency to use greywater for irrigation, it is interesting to note that the current research is very limited on how vadose zone flow is affected by different types of surfactants. Surfactants, even in low concentrations, are able to decrease the surface tension and thus affect soil capillarity within the vadose zone according to Equation 1 (Bear, 1972),

$$\psi = -\frac{2\sigma\cos(\gamma)}{\rho gr} \quad [1]$$

where ψ is soil water pressure head, σ is surface tension, γ is effective contact angle, ρ is density of the solution, g is the gravitational acceleration and r is the effective pore radius. Surfactant induced unsaturated flow refers to the tendency of flow to take place even at similar water contents, from the surfactant contaminated regions towards uncontaminated regions, because of the pressure gradients, which are formed due to the differences in surface tension (Smith and Gillham 1999). Since surfactants lead to a decrease in surface tension and associated capillary forces for similar gravitational forces, it is reasonable to expect an infiltration pattern with a decrease in horizontal spreading and an increase in vertical penetration, in comparison to the pure water case. However, a numerical modeling study by Henry and Smith (2006), indicates that in instances a surfactant solution is infiltrated into the vadose zone there is a significant horizontal increase and a minor vertical decrease in flow.

Based on the results of their experimental and numerical models, Smith et al. (2011) noted the formation of a capillarity-induced focused flow (SCIFF) region, as a consequence of clean water infiltration into vadose zone with surface active solute contamination. Constrained by the surfactant induced pressure gradients in the horizontal direction, pure water is forced to move within a single finger-patterned, highly focused, vertical flow. Smith et al. (2011) also note that the SCIFF mechanism is expected to be valid for any organic compound contamination cases in vadose zone.

Henry et al. (2002) studied the infiltration of a surface active solute in a two dimensional (2D) flow cell. They also simulated their experimental data using a modified version of Hydrus 2D (Simunek et al. 1999). Concentration dependent surface tension and viscosity effects were implemented in the modified version of Hydrus 2D. The differences between experimental and numerical results were attributed to the lack of hysteretic hydraulic functions in the numerical model. Although changes in water content is generally associated with non-monotonic boundary conditions; surfactant infiltrations, which lead to pressure gradients due changes in surface tension, cause hysteresis to have an important effect on vadose zone flow and transport characteristics, even under monotonic flow conditions. Bashir et al. (2009) modified the hysteresis routine of HYDRUS-2D and simulated Henry et al. (2002)'s experimental data. Successful implementation of hysteresis in hydraulic functions provided a better correlation between the experimental data and numerical results. They concluded that hysteresis plays an important role in accurate depiction of surfactant affected unsaturated flow and transport systems.

1-Butanol and Triton X-100 have been used as model surfactants in many experimental and numerical studies of surfactant affected unsaturated flow systems (Smith and Gillham, 1999; Henry et al., 2002; Smith et al., 2011; Karagunduz et al., 2001; Karagunduz et al., 2015). Butanol is a widely used solvent mainly in household products and for personal care and medical purposes. Bashir et al (2018) point out that butanol has a few health and safety risks with a very low Henry's partitioning coefficient, which raises no concern for vapor transport. In addition, Butanol does not readily sorbs to soils. Depending upon the concentration,

Butanol can depress the surface tension of water from 72 mN/m to 24.8 mN/m. Moreover butanol does not alter the contact angle.

Triton X-100 is a non-ionic surfactant, which is generally used as an ingredient in household and industrial cleaners, paints and coatings. Triton X-100 is soluble in water and chemically stable in most acidic and alkaline solutions (The DOW Chemical Company, 2018).

Concentration dependent surface tension effects of both butanol and Triton X-100 have been studied in experimental and numerical studies. However, there is no evidence in the peer review literature that a systematic comparison of flow and transport of two surfactants has been carried out. Such a comparison is important considering some important differences. For example the maximum depression of surface tension for butanol is achieved at a concentration of 70 mg/L which also results in significant viscosity changes. In comparison maximum depression of surface tension for Triton X-100 can be achieved at mere concentration of 0.15 mg/L with no viscosity effects. More importantly Triton X-100 sorbs to the soil particles and modifies the contact angle, while butanol does not do so. Additionally there are no experimental or numerical studies on flow and transport of Triton X-100 in 2D domains.

In this research, a modified version of Hydrus 2D, was used to compare and contrast the infiltration of pure water with conservative tracer to that of infiltration of butanol and Triton X-100. Infiltration assessment was done for a fine sand at its residual moisture content. Concentration dependent surface tension and viscosity effects were implemented to simulate butanol infiltration by coupling flow and transport processes. Similarly concentration dependent surface tension, contact angle, and sorption effects for Triton X-100 were also implemented in the numerical model. This is the very first implementation of its type in a 2D flow and transport model.

Results indicate that surfactant solutions led to notable differences in flow and transport in comparison to pure water. Also, infiltration behavior of Butanol and Triton X-100 differed significantly due to their different sorption characteristics.

2 METHODOLOGY

Hydrus 2D (Simunek et al. 1999), a two dimensional finite element software, uses a mixed form of Richards' equation (Equation 2) for water transport flow in variably saturated soils.

$$\frac{\partial \theta}{\partial t} = \frac{\partial}{\partial x_i} \left[K \left(K_{ij}^A \frac{\partial \psi}{\partial x_j} + K_{ij}^A \right) \right] \quad [2]$$

In Equation 2, θ is volumetric moisture content, t is the time, i and j are indices which are from 1 to n , x_i is spatial coordinate, ψ is pressure head, K_{ij}^A is the component of a dimensionless anisotropy tensor (K^A) and K is the unsaturated hydraulic conductivity function, given by Equation 3.

$$K(\psi, x, z) = K_s(x, z)K_r(\psi, x, z) \quad [3]$$

where, K represents unsaturated hydraulic conductivity function, K_r represents relative hydraulic conductivity function, and K_s represents saturated hydraulic conductivity value.

The soil used for this study is a 120-mesh silica sand previously used by Henry et al. (2002) and Bashir et al. (2009). Main drainage and wetting data were fitted to the van Genuchten equation (1980) as given in Equation 4,

$$\theta = \frac{\theta_s - \theta_r}{(1 + |\alpha\psi|^n)^{(1-\frac{1}{n})}} + \theta_r \quad [4]$$

where α and n are curve fitting parameters, θ_s is the saturated volumetric water content and θ_r is the residual water content. Soil water characteristic curve parameters were taken as follows: $\theta_s = 0.270$, $\theta_r = 0.0449$, $\alpha_{drainage} = 0.015$, $\alpha_{wetting} = 0.021$ and $n = 11.2$.

In order to solve the water flow equation, it is important to consider the effects of the solute concentration on surface tension and contact angle which has a concomitant impact on pressure head (Equation 1). Changes in surface tension and contact angle can be taken into account by scaling the pressure head in the van Genuchten equation as follows.

$$\psi^* = \frac{\sigma_o \cos \gamma_o}{\sigma(c) \cos \gamma(c)} \psi \quad [5]$$

In Equation 5, ψ^* represents the solute concentration dependent pressure head, whereas ψ represents the pressure head without any solutes at $c_o = 0.0$. σ_o is the surface tension and γ_o is the contact angle at the reference concentration, both at $c_o = 0.0$, while $\sigma(c)$ and $\gamma(c)$ are the surface tension and contact angle, both at solute concentration c . Substituting Equation 5 in Equation 4 enables the calculation of solute concentration effects by using the scaled version of the van Genuchten equation (1980), as given in Equation 6.

$$\theta = \frac{\theta_s - \theta_r}{(1 + |\alpha\psi^*|^n)^{(1-\frac{1}{n})}} + \theta_r \quad [6]$$

It is important to note that, biodegradation and vapor phase partitioning properties are neglected in this study. Additionally, sorption characteristics were taken into account only for only Triton X-100, as butanol sorption to soil is negligible.

Hydrus 2D solves Equation 7 to simulate the solute transport in vadose zone,

$$\frac{\partial \theta C_a}{\partial t} + \frac{\partial \rho S_a}{\partial t} = \frac{\partial}{\partial x_i} \left(\theta D_{ij} \frac{\partial C_a}{\partial x_j} \right) - \frac{\partial q_i C_a}{\partial x_i} \quad [7]$$

where C_a is the concentration of the solute a , S_a is the sorbed phase concentration of solute a , q is the Darcy flux, ρ is the bulk density and D_{ij} is the hydrodynamic dispersion coefficient tensor.

Hydrodynamic dispersion coefficient is calculated using Equation 8,

$$\theta D_{ij} = D_T |q| \delta_{ij} + (D_L - D_T) \frac{q_i q_j}{|q|} + \theta D_w \tau_w \delta_{ij} \quad [8]$$

where D_w is the free water molecular diffusion coefficient, τ_w is the liquid phase tortuosity factor, δ_{ij} is the Kronecker delta function, D_L is the longitudinal and D_T is the transverse dispersivity.

Hydrus 2D calculates the liquid phase tortuosity factor using Millington and Quirk (1961) relationship, as given in Equation 9.

$$\tau_w = \frac{\theta^{7/3}}{\theta_s^2} \quad [9]$$

2.1 Butanol Scaling Relationships

Smith and Gillham (1994) used Equation 10, to take into account the effect of concentration on pressure head for butanol. It is important to highlight that scaling for butanol concentration is solely based on the changes in surface tension, as butanol concentration has negligible effect on contact angle.

$$\frac{\psi}{\psi^*} = 1 - b \ln \left(\frac{c}{a} + 1 \right) \quad [10]$$

In Equation 10, a and b are solute dependent constants. σ is the surface tension at concentration c , whereas σ_o represents the surface tension at the reference concentration, c_o . Substituting Equation 10 into Equation 5 scaled SWCC for butanol can be obtained. The scaled soil moisture characteristic curve for 7% w/w butanol solution are shown in Figure 1.

Since hydraulic conductivity function is dependent on changes in kinematic viscosity, a scaled version of Mualem (1976) equation can be used to consider the solute effects on unsaturated hydraulic conductivity for butanol.

$$K(\theta, c) = \frac{v}{v_o} K_s \theta^l \left(1 - \left(1 - \theta^{\frac{1}{m}} \right)^m \right)^2 \quad [11]$$

In Equation 11, l and m are curve fitting parameters. $K(\theta, c)$ represents the concentration dependent unsaturated hydraulic conductivity, K_s represents the pure water saturated hydraulic conductivity and θ represents pure water effective saturation.

$$\frac{v}{v_o} = \left(1 - e \ln \left(\frac{c}{a} + 1 \right) \right)^{-1} \quad [12]$$

Equation 12 was proposed by Smith and Gillham (1999) in order to calculate the kinematic viscosity changes due to surfactant concentration. In Equation 12, d and e are solute dependent constants. v is the kinematic viscosity at concentration c , and v_o represents viscosity at the reference concentration c_o . Kinematic viscosity of the pure water with zero concentration of surfactants is $v_o = 0.9017$ cSt at $c_o = 0.0$.

According to Bashir et al. (2018), for a 7% w/w butanol solution at 25°C, constants a , b , d and e are determined to be 0.365, 0.215, 34.49 and 1.366, respectively.

2.2 Triton X-100 Scaling Relationships

Karagunduz et al. (2015) used Triton X-100 and conducted experimental and numerical tests to investigate its effects on soil water retention curve. They conducted column and batch reactor experiments with F-70 Ottawa Sand (40-270 mesh). They also simulated the experiment using a modified version of Hydrus 1-D.

Similar to Smith and Gillham (1994), Karagunduz et al. (2015) also used a scaled version of van Genuchten equation to consider Triton X-100 concentration effects. Equation 13 shows the pressure head scaling parameters for Triton X-100, which addresses both the surface tension and contact angle changes due to surfactant concentration.

$$\frac{\psi}{\psi^*} = \frac{1}{(1 + \beta C_s)} \quad [13]$$

In Equation 13, β represents a solution specific scaling factor and C_s is the surfactant concentration. Karagunduz et al. (2015) used a β value of 0.0047 L/mg for Triton X-100. Substituting Equation 13 into Equation 5 gives the scaled van Genuchten equation for Triton X-100 in the form of Equation 4. The scaled soil moisture characteristic curve for Triton X-100 solution at its critical micelle concentration can be seen in Figure 1.

Surfactants stay as monomers at low concentrations but as their concentration increases, they start to form micelles. The concentration, where the solution properties change from monomers to micelles are defined as critical micelle concentration (CMC). CMC is commonly measured using the surface tension and can be defined as the break point, where surface tension remains constant with further increase in concentration (Tadros, 2013). In their earlier work, (Karagunduz et al., 2001), concluded that once the surfactant concentration reaches critical micelle concentration (CMC), which is 150 mg/L for Triton X-100, C_s and consecutively $(1 + \beta C_s)$, reaches its maximum and does not change with increasing concentration.

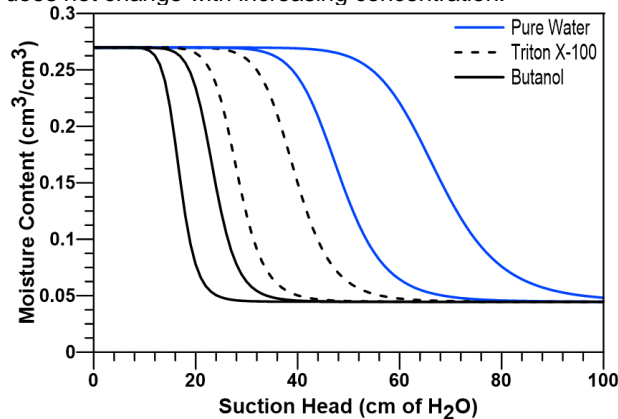


Figure 1 Soil-water characteristic curves for pure water, Triton X-100 at its critical micelle concentration (CMC) and 7% w/w butanol solutions.

Unlike butanol, sorption is an important trait of Triton X-100, which affects the flow and transport properties.

$$s = \frac{k_s c}{1 + \eta c} \quad [14]$$

Hydrus 2D uses Equation 14 to define Langmuir adsorption relationship, where s is adsorbed concentration, c is the solution concentration, and k_s and η are solute dependent empirical coefficients.

Based on the results of the conducted batch reactor experiments provided in Karagunduz et al. (2015), input Langmuir adsorption equation parameters for our Hydrus 2D model were fitted as $k_s = 0.613$ and $\eta = 10.65$.

3 MODELING

A 680 cm wide and 550 cm high rectangular domain of porous medium, which Henry and Smith (2006) proved to be large enough to prevent flow effects to extend to the right or left boundaries, was used for the numerical simulation. Bashir et al. (2018) modelled a numerical experiment which can be related to in-situ conditions, where an unsaturated soil experiences drying and wetting cycles due to irrigation and evaporation. In this study, the same modeling characteristics were used, which enable the numerical investigation of the hysteretic flow behavior of different surfactants under intermittent boundary conditions. For numerical experiments of Butanol and Triton X-100, the left and right boundaries of the domain were defined as no flow conditions. Additionally, a unit vertical hydraulic gradient along the bottom boundary was defined to simulate free drainage. Top boundary was also defined with no-flow boundary condition except for the center 1.9 cm portion, where a point variable flux source was assumed. The top variable flux boundary was defined to go through four periodic 24 hours changes, as defined in Table 1. A Cauchy type solute boundary condition with a relative concentration of 1.0 was applied for the first 24 hour period.

In order to maintain no ponding condition at the surface, for both of the periods, infiltration rates (0-24 hours and 48-72 hours) were chosen to be less than soil hydraulic conductivity. The initial condition of pressure head was defined as -300 cm of head to keep the porous media at its residual moisture content. Applied intermittent flux boundary conditions are outlined in Table 2.

Table 1. Applied Intermittent Periods and Definitions

Time (Hours)	Definition
$0 < t \leq 24$	First infiltration period. Pure water, Butanol or Triton X-100 solutions was applied for 24 hours. This part simulates the application of surfactant solution either for agricultural irrigation or subsurface remediation purposes.
$24 < t \leq 48$	First redistribution period. No infiltration was applied for 24 hours. The infiltrated solution was allowed to redistribute.
$48 < t \leq 72$	Second infiltration period. Pure water was introduced to the system for all three cases. This condition simulates when a precipitation event follows the surfactant solution application.
$72 < t \leq 96$	Second redistribution period. No infiltration was applied for 24 hours and again, redistribution took place.

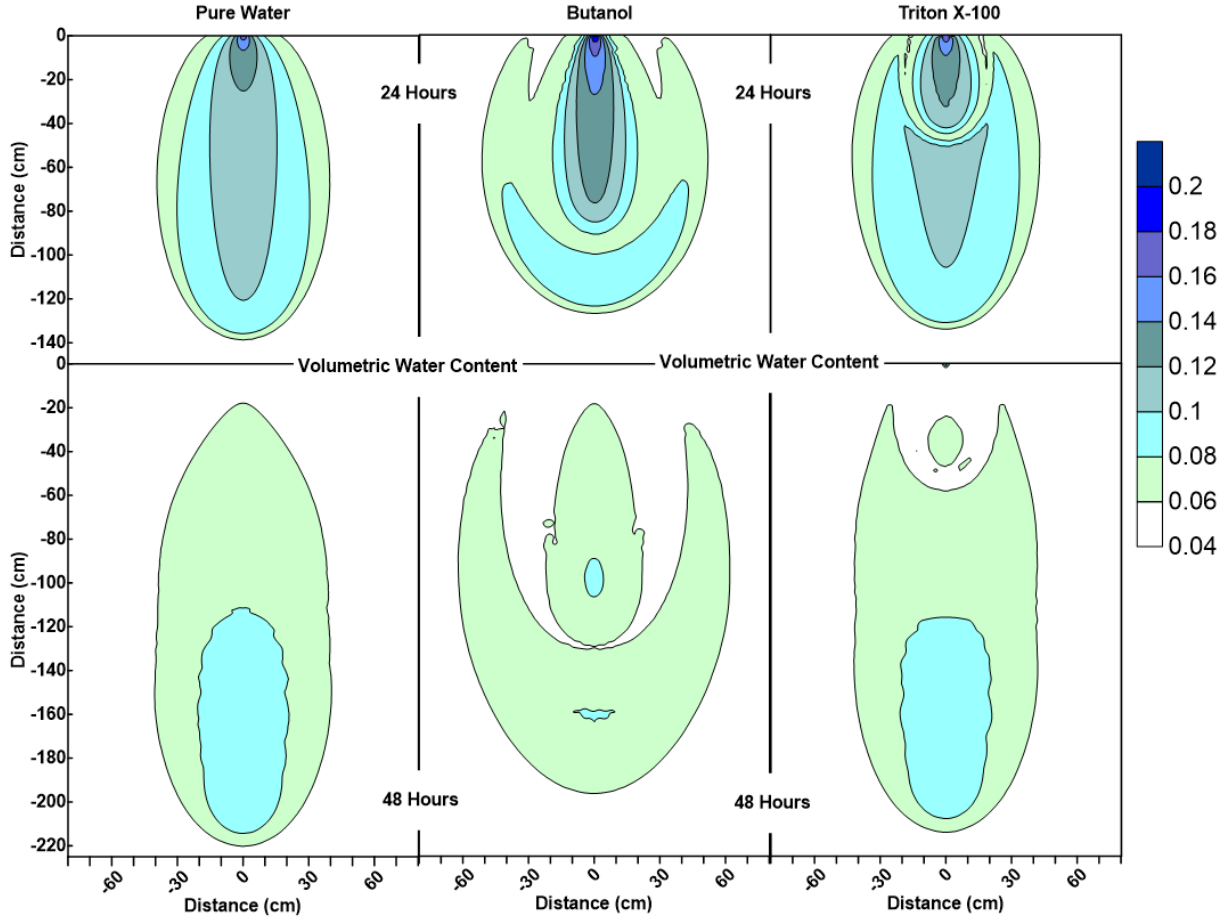


Figure 2: Water content profiles at 24 and 48 hours for pure water, Butanol and Triton X-100 solutions
 Note: The numerical results for Pure Water and Butanol were adapted from Bashir et al (2018).

Table 2. Applied Intermittent Flux Boundary Conditions

Surface Flux Condition	t (hours)	$q_o(cm/hr)$	C/C_o
Infiltration	$0 < t \leq 24$	8.875	1.0
Redistribution	$24 < t \leq 48$	0.0	0.0
Infiltration	$48 < t \leq 72$	8.875	0.0
Redistribution	$72 < t \leq 96$	0.0	0.0

4 RESULTS

As surfactants decrease the surface tension, it has been hypothesized that the solution would infiltrate deeper due to lower capillary forces for similar gravitational forces. The results of this numerical experiment support the earlier observations by Henry and Smith (2006) and Bashir et al. (2018), that this is not the case. Figure 2 and Figure 3 shows the water content and concentration profiles for 24 and 48 hours after first infiltration and redistribution periods. Figure 2 shows that, for both of the surfactant infiltration cases, the depth of wetted zone decreased slightly and enhanced horizontally at both 24 hours and 48

hours. The depth and width of the wetting front are tabulated data in Table 3 and Table 4

Table 3. Comparison of Maximum Wetted Penetrations for Water and Different Types of Surfactants

Maximum Wetted Penetration (cm) at	Water	Butanol	Triton X-100
24 hours	140	127	135
48 hours	220	196	214
72 hours	270	281	264
96 hours	326	386	345

Table 4. Comparison of Maximum Lateral Spreading for Water and Different Types of Surfactants

Maximum Lateral Spreading(cm) at	Water	Butanol	Triton X-100
24 hours	80	102	85
48 hours	80	124	85
72 hours	88	120	95
96 hours	100	112	103

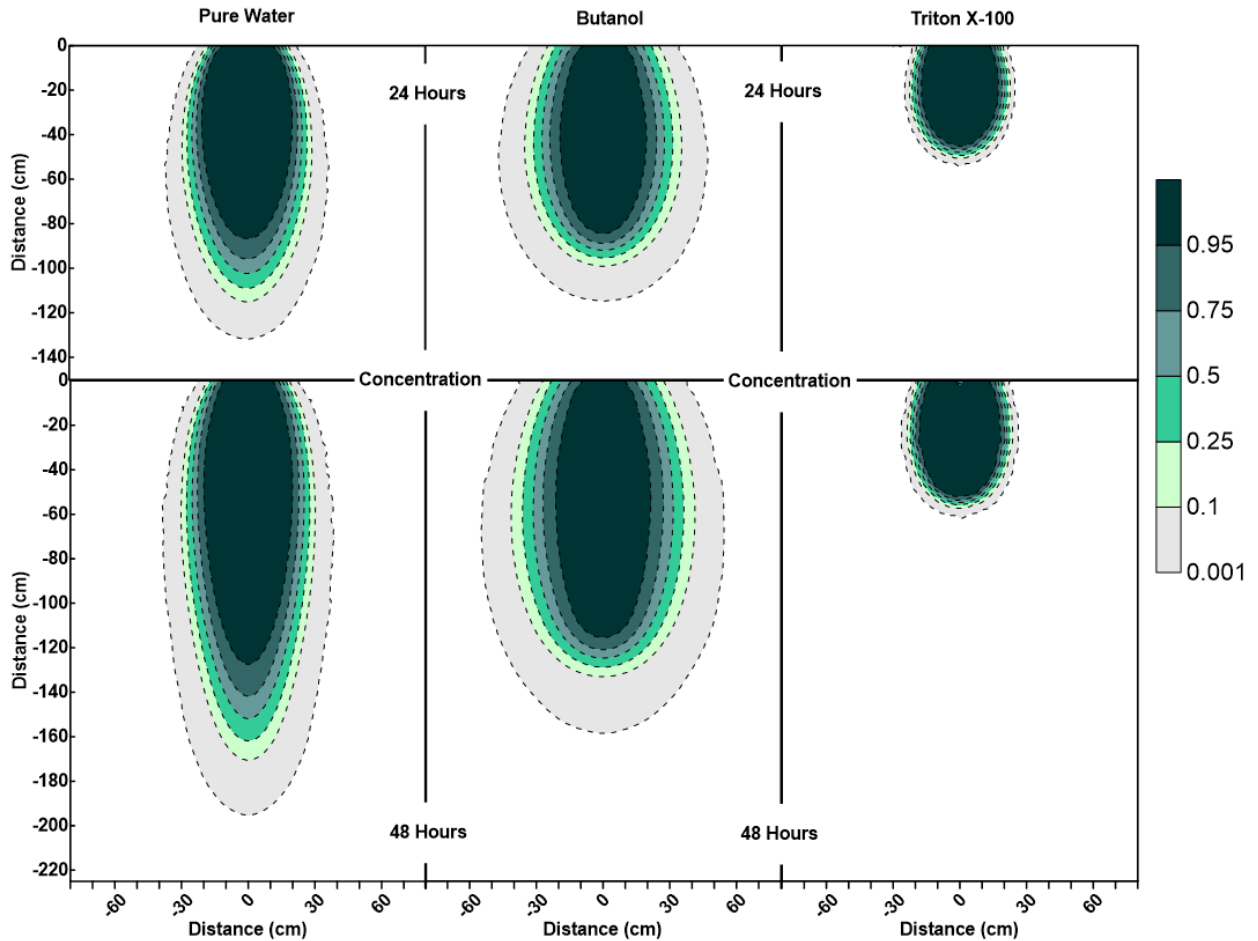


Figure 3: Concentration profiles after 24 and 48 hours for pure water, Butanol and Triton X-100 solutions
 Note: The numerical results for Pure Water and Butanol were adapted from Bashir et al (2018).

Another important feature that surfactant infiltration is the development of desaturated zone behind the wetting front. This is attributed to the fact that surfactants reduce the water holding capacity of the sand as result of reduction of surface tension. It can also be observed that the depth of the desaturated zone is much shallower in the case of Triton X-100. This correlates well with the location of Triton X-100 in the system as it can be observed that most of the surfactant is located in the top 40 cm of the domain.

At the end of the first redistribution period, at 48 hours, it was observed that Triton X-100 did not go through lateral spreading to the same extent as Butanol. Volumetric water content profile pattern of Triton X-100 can be defined as a combination of the behavior of pure water with conservative tracer and Butanol cases, as can be seen in Figure 2, Table 3 and Table 4.

Figure 4 and Figure 5 shows the volumetric water content and concentration profiles for 72 hours and 96 hours. The volumetric water content profiles for surfactants clearly indicate the development of SCIFF. However the SCIFF region for Triton X-100 is much shallower. This once again is result of the presence of most of Triton X-100 at shallower depth as shown in the concentration profile.

The concentration profiles shown in Figure 5, indicate that infiltration of clean water infiltration in surfactant

contaminated systems was not successful to flush the surfactants out from the system. This was due the SCIFF phenomena (Smith et al., 2011), predominantly observed in Butanol case, which resulted in larger vertical displacement of water with a very small portion horizontal displacement. For Triton X-100, we see a shorter SCIFF region within the 20 cm to 80 cm depth and for deeper sections the behavior is again in resemblance with the pure water case.

After the second redistribution period at 96 hours, Figure 5 and Table 3 show that, more vertical water movement was observed in surfactant cases, when compared to the pure water case. At the end of the fourth day, it is important to highlight the movement in the concentration profile of the pure water case, where most of the concentration shifted to 120 cm depth; while for Butanol and Triton X-100 cases, concentration profile was less affected and surfactants still resided in the surface soil layers. This behavior is very obvious for Triton X-100 case, where the concentration profiles were very similar at 72 hours and 96 hours and the surfactant was able to penetrate only to 90 cm depth (around one third of penetration that is experienced by Butanol), due to sorption.

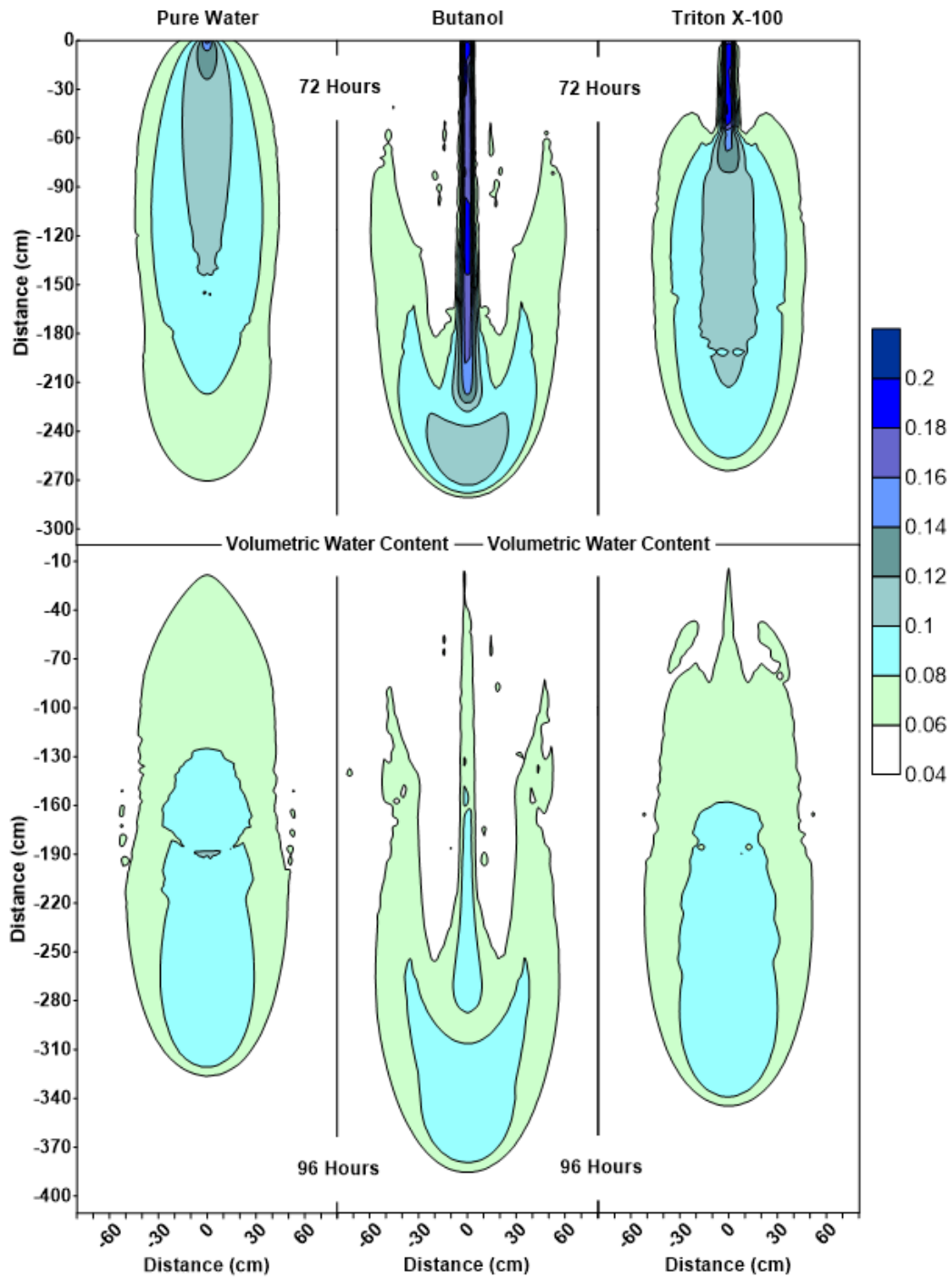


Figure 4: Volumetric water content profiles after 72 and 96 hours for without surfactant, Butanol and Triton X-100 solutions
 Note: The numerical results for Pure Water and Butanol were adapted from Bashir et al (2018).

5 CONCLUDING REMARKS

This numerical study compares the infiltration characteristics of two surfactants (Butanol and Triton X-100) and water in an unsaturated porous medium with a deep water table under intermittent flux boundary conditions. The numerical study was carried out using a modified version of Hydrus 2D in which concentration

dependent surface tension, viscosity, contact angle and sorption effects were implemented.

The results of this study show that Butanol and Triton X-100 infiltration lead to complex flow patterns and change the hydraulic characteristics of unsaturated porous medium. These surfactant specific changes are due to the concentration dependent surface tension, contact angle, viscosity and sorption effects.

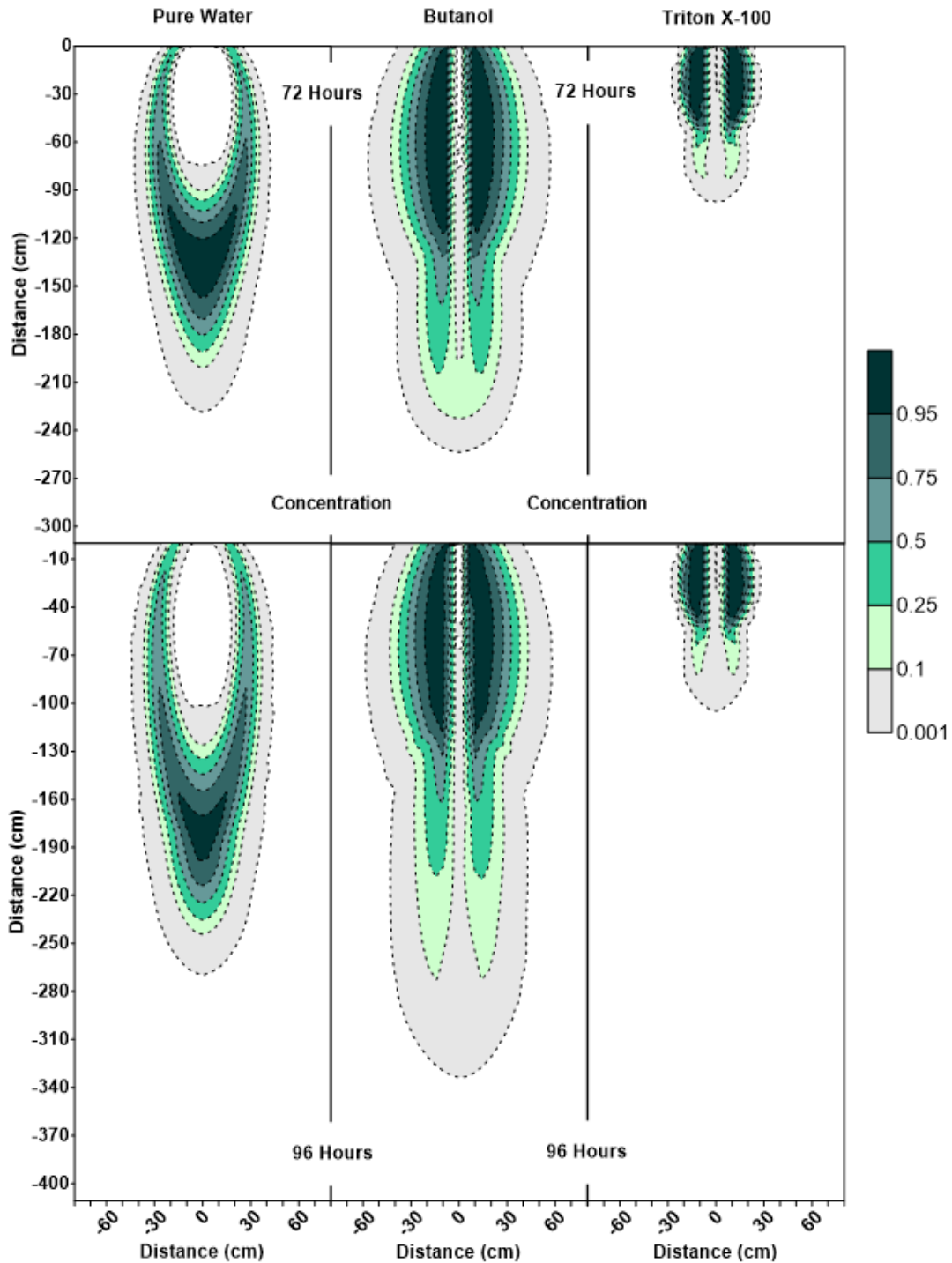


Figure 5: Concentration profiles after 72 and 96 hours for without surfactant, Butanol and Triton X-100 solutions
 Note: The numerical results for Pure Water and Butanol were adapted from Bashir et al (2018).

First infiltration period results reveal that surfactants lead to a shorter and wider water content and concentration profiles. Profiles after the first redistribution period show that surfactant contamination causes enhanced lateral spreading and reduced depth of the wetting front. The presence of surfactants also results in reduction of water holding capacity of the sand resulting in lower saturation regions in the areas of higher surfactant concentration. It

was also observed that surfactant sorption plays an important role and led to a small and highly concentrated contaminated area near the point of application for Triton X-100 solution. This accumulation at shallower depth leads to a much smaller SCIFF region.

Results of water infiltration and redistribution periods within the 48 hours - 96 hour periods, emphasizes the important impact of SCIFF zone, which confines the flow

within a narrow area with an intense water movement in the vertical direction. Comparison of conservative tracer with the surfactant cases clearly shows that, this focused flow area is far from sufficient to flush the surfactant out from the system. Real life implications of this numerical simulation suggest that pure water infiltration after surfactant infiltration could intensify the vertical water movement within the area of application, hindering the plant roots to get sufficient water, as also pointed out by Bashir et al (2018). Additionally, for vadose zone surfactant infiltration cases, even if the system was flushed with clean water afterwards, surfactant accumulation near the surface soil layers should be expected. Considering the surfactants used in this study, surfactant accumulation profiles are dominantly affected by the surfactant sorption characteristics.

All of the above mentioned changes highlight the need and importance of considering the surfactant concentration effects, in order to make accurate predictions of the flow and transport of surfactants in the vadose zone. Outcomes of this study are beneficial to understand the effects of surfactant contaminated greywater in vadose zone as well as designing soil and ground water remediation solutions using surfactants.

REFERENCES

- Abu-Zreig, M., Rudra, R. P., & Dickinson, W. T. (2003). Effect of Application of Surfactants on Hydraulic Properties of Soils. *Biosystems Engineering*, 84(3), 363–372. [https://doi.org/10.1016/S1537-5110\(02\)00244-1](https://doi.org/10.1016/S1537-5110(02)00244-1)
- Bashir, R., Smith, J. E., Henry, E. J., & Stolle, D. (2009). On the Importance of Hysteresis in Numerical Modeling of Surfactant-Induced Unsaturated Flow. *Soil and Sediment Contamination: An International Journal*, 18(3), 264–283. <https://doi.org/10.1080/15320380902772638>
- Bashir, Rashid, Smith, J. E., & Stolle, D. F. (2018). Surfactant Flow and Transport in the Vadose Zone: A Numerical Experiment, *Environmental Geotechnics*, ICE Publishing. <https://doi.org/10.1680/jenge.17.00090>
- Bear, J. (1972). *Dynamics of fluids in porous media*. New York: Dover.
- Eriksson, E., Auffarth, K., Eilersen, A.M., Henze, M., Ledin, A. (2003). Household chemicals and personal care products as sources for xenobiotic organic compounds in grey wastewater. *Water SA* 29, 135–146.
- Henry, E. J., & Smith, J. E. (2006). Numerical demonstration of surfactant concentration-dependent capillarity and viscosity effects on infiltration from a constant flux line source. *Journal of Hydrology*, 329(1), 63–74. <https://doi.org/10.1016/j.jhydrol.2006.02.008>
- Henry, E. J., Smith, J. E., & Warrick, A. W. (2002). Two-dimensional modeling of flow and transport in the vadose zone with surfactant-induced flow Henry EJ, Smith JE and Warrick AW . *Water Resources Research*, 38(11): 33.1–33.16.
- Karagunduz, A., Pennell, K. D., & Young, M. H. (2001). Influence of a Nonionic Surfactant on the Water Retention Properties of Unsaturated Soils. *Soil Science Society of America Journal*, 65(5), 1392–1399.
- Karagunduz, A., Young, M. H., & Pennell, K. D. (2015). Influence of surfactants on unsaturated water flow and solute transport. *Water Resources Research*, 51(4), 1977–1988. <https://doi.org/10.1002/2014WR015845>
- Mualem, Y. (1976). A new model for predicting the hydraulic conductivity of unsaturated porous media. *Water Resources Research*, 12(3), 513–522. <https://doi.org/10.1029/WR012i003p00513>
- Simunek, J., Sejna, M., & van Genuchten, M. T. (1999). *The HYDRUS-2D Software Package for Simulating the Two-Dimensional Movement of Water, Heat, and Multiple Solutes in Variably-Saturated Media, Version 2.0*. Int. Ground Water Model. Cent., Colo. Sch. of Mines, Golden, Colorado.
- Smith, J. E., Henry, E. J., & Bashir, R. (2011). Solute-Dependent Capillarity-Induced Focused Flow during Infiltration into Alcohol-Contaminated Soil. *Vadose Zone Journal*, 10(1), 403. <https://doi.org/10.2136/vzj2009.0081>
- Smith, J., & W. Gillham, R. (1994). The effect of concentration-dependent surface tension on the flow of water and transport of dissolved organic compounds: A pressure head-based formulation and numerical model. *Water Resources Research - WATER RESOUR RES*, 30, 343–354.
- Smith, J., & W. Gillham, R. (1999). Effects of solute concentration-dependent surface tension on unsaturated flow: Laboratory sand column experiments. *Water Resources Research - WATER RESOUR RES*, 35.
- Tadros, T. (2013). Critical Micelle Concentration. In T. Tadros (Ed.), *Encyclopedia of Colloid and Interface Science* (pp. 209–210). Berlin, Heidelberg: Springer Berlin Heidelberg. https://doi.org/10.1007/978-3-642-20665-8_60
- The DOW Chemical Company. (2018, April 22). TRITON™ X-100 Surfactant. Retrieved from https://www.dow.com/assets/attachments/business/pcm/triton/triton_x-100/tds/triton_x-100.pdf
- Van Genuchten, M. (1980). A Closed-form Equation for Predicting the Hydraulic Conductivity of Unsaturated Soils. *Soil Science Society of America Journal*, 44.
- Wiel-Shafran, A., Ronen, Z., Weisbrod, N., Adar, E., & Gross, A. (2006). Potential changes in soil properties following irrigation with surfactant-rich greywater. *Ecological Engineering*, 26(4), 348–354. <https://doi.org/10.1016/j.ecoleng.2005.12.008>